Development of Lunar or Planetary Subsurface Exploration Robot Using Peristaltic Crawling

Chuo University
Hayato Omori

【Introduction】

Aerospace exploration has great potential to lead to new discoveries, such as new substances, or help find keys to the origin of our planet. Planetary and asteroid investigations have provided basic information about the planets, such as geological, magnetic, and gravitational properties. Many explorers and robots have been placed on their surfaces for these reasons. All this remains very limited though. Small unmanned explorers will be needed first, both for safety and economic reasons. As a small unmanned subsurface explorer robot, Richter et al. [1] developed the planetary underground tool (PLUTO) with a diameter of 20 mm, a length of 280 mm and a mass of 0.35 kg. It was able to excavate to a depth of 2 m. Stoker et al. [2] then developed the Moon Mars underground mole (MMUM) with a diameter of 40 mm and a mass of 2 kg. MMUM could reach a depth of approximately 500 mm in the 30 grit silica dry-sand. Honeybee Robotics and NASA-JPL [3] have developed the Auto-Gopher with an outer diameter of 71 mm a length of 1.8 m and a mass of 22 kg. It could excavate to a depth of 3 m in the hard Gypsum but it is made for drilling a hard material. Both a mole type robot [4] and a screw type robot [5], which are more than 100 mm in diameter, have been developed. However, these explorers are only able to excavate to the depths of tens of centimetres in regolith stimulant. These 4 types of excavators (excluding the Auto-Gopher because it is for drilling a hard material) indicate that it becomes more difficult to perform deep excavations as the diameter of the robot increases. Because of the effect of earth pressure in the surrounding material, excavators are not able to generate enough pushing force on the front material [4]. Moreover, it is difficult to make a front space for propulsion [6]. Yasuda et al. have developed a second prototype of the self-turning screw mechanism (STSM) [7], which has a diameter of 120 mm, a length of 632 mm and a mass of 11.6 kg. The robot was able to drill to a depth of 812.6 mm in fly ash, while 1/6th of its own weight through use of counterweights to simulate the smaller gravity on the Moon relative to the Earth. However, it consumes 100 W of power.

This paper describes the development of a small lunar and planetary subsurface explorer robot, which has propulsion and excavation units based on the locomotion mechanism of an earthworm and an earth auger (EA), respectively. First, a prototype robot was developed with a propulsion unit and an excavation unit. Then a discharging part was improved for deep excavation. Finally, basic cutting experiments with the front of the excavation unit were carried out to provide data for excavation models.

【Concept of a Novel Subsurface Explorer Robot】

The robot consists of two elements: a propulsion unit and an excavation unit (see Fig. 1). The peristaltic crawling behavior of an earthworm is adopted as the motion principle for the propulsion unit, and an EA is chosen as an excavation tool. The propulsion unit of the robot consists of four subunits corresponding to the individual segments of an earthworm. Fig. 2 shows their functioning while performing a peristaltic motion. Each subunit can contract and extend in the axial direction, and expand in the radial direction while contracting in the axial direction, thereby ensuring a high degree of friction between the body of the robot and its surroundings. Conversely, units that are extended in the axial direction do not make contact with their surroundings. The excavation unit of our prototype robot includes an EA with three parts allowing the following specific duties: excavation, transport, and discharge. The EA digs the hole, the front

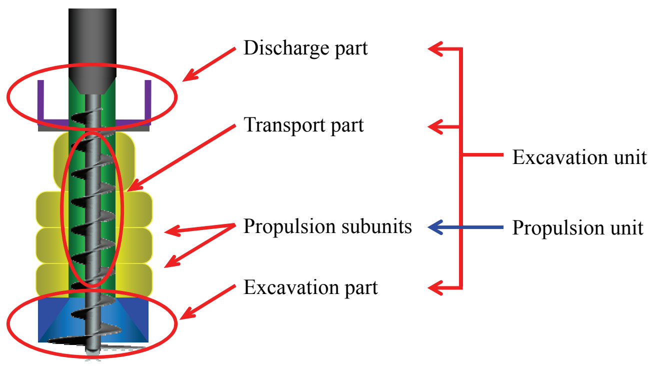

Fig.1 Concept of the robot

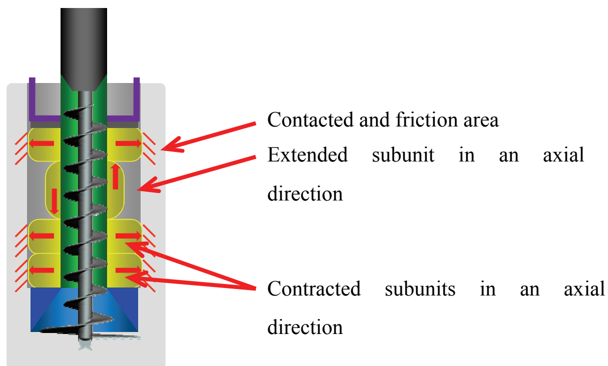

Fig.2 Functioning of propulsion subunits inside a hole

part excavates the material, and the screw part transports the excavated material to the rear of the EA, where it is discharged in a bucket. When the bucket is filled with the discharged material, it is lifted to transport and discharge to the surface. The material is discharged and the bucket becomes empty. The empty bucket returns to the end of the robot. The robot excavates underground by making full use of these mechanisms.

【Development of a Subsurface Explorer】

Fig. 3 shows the excavation and propulsion units combined to form the developed robot. It consists of four propulsion subunits, each of which has four expansion plates. Additional rubber friction sheets are placed on the outer surface of the expansion plates, which increase the friction forces while the robot is moving inside a launcher. These plates cover a large area of the outer surface of the unit. The remaining uncovered spaces, i.e., the gaps between the propulsion units and those between expansion plates are covered with dirt proof material (aluminium evaporation sheets) to prevent soil from getting inside the subunits. The excavation unit connects to the front of the propulsion unit, and the transport part passes through, inside the propulsion subunits. A DC motor located at the rear end of the robot powers the EA. The excavated soil is discharged from discharge ports behind the propulsion unit. The total mass of the prototype robot is 5.28 kg and its length is 800 mm.

For possible future missions, the excavator could operate on the Moon or other bodies with a gravity six times less intense than that of the Earth. The developed device has been tested in excavation experiments in similar, lighter weight conditions by using counterweights. The forces applied to the EA were set at 1/1, 1/2 (26 N), 1/4 (13 N) and 1/6 (8.7 N) of its own weight on Earth of 52 N. The propulsion velocity of the robot was set at 0.25 mm/s.

Fig. 4 shows the experimental process. This process can be described in six phases, as follows: (a) Beginning of the experiment. (b) Discharge ports reaching Stage 3. (c) Stage 3 of the launcher separated to both sides. (d) After Stage 2 separation. (e) After Stage 1 separation. (f) Excavation stopped when discharge ports reached soil level.

Fig. 5 shows the experimental results in terms of depth of excavation and motor torque as functions of time. As shown in this figure, the excavation velocity mainly changed at approximately 9 minutes when the robot was released from the top stage of the launcher. Then, for 1 or 2 minutes, the velocity became faster than that prior to this 9 minutes mark. The motor torque also increased because of this slip. At this point, the front subunit was moving in the soil and the other subunits were moving in the launcher. It assumes that it was difficult to generate enough friction force because the surface of shallow soil was weak and not packed. Excavation remained constant until the bottom stage of the launcher was released. From this point on, the robot continued excavating although the velocity decreased. The hole and the robot

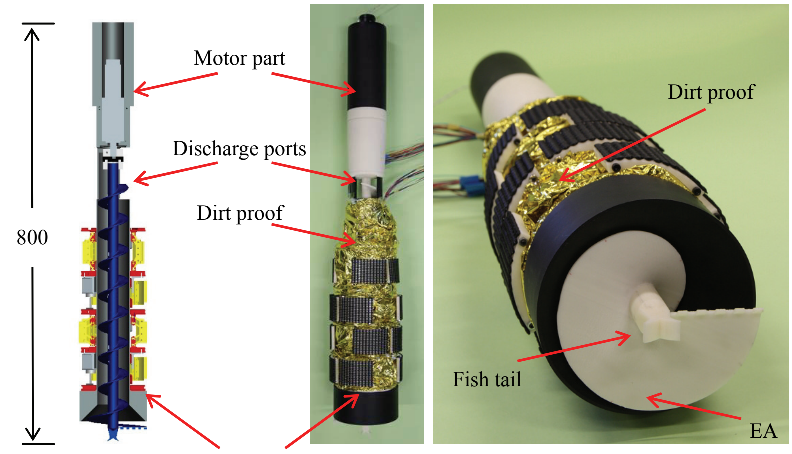

Fig. 3 Developed robot with excavation and propulsion

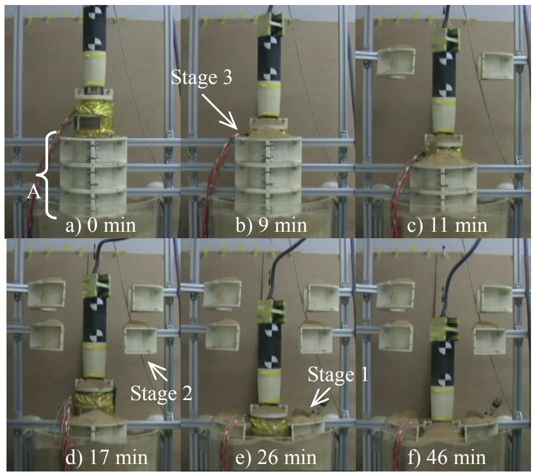

Fig. 4 Excavation experiments with launcher (A: Launcher)

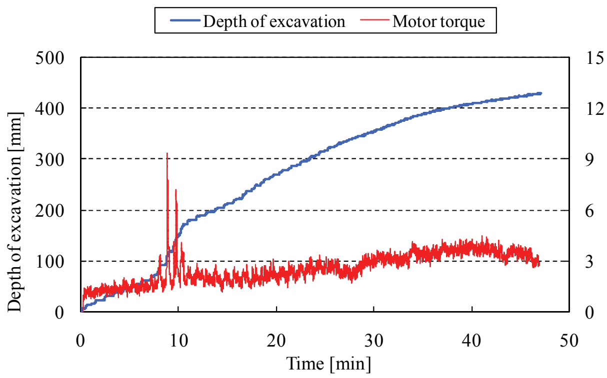

Fig. 5 Results of excavation (52 N)

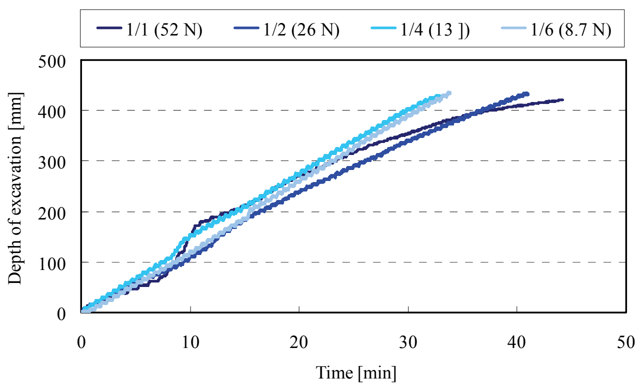

Fig. 6 Experimental results of different weights of the excavator

were investigated after excavation. It seemed that the discharged soil fell into the hole, preventing the propulsion unit from working properly. The results for the new robot, with both units integrated, clearly depict a stair shape in Fig. 5, and the robot did not just fall down through the hole under its own weight, but succeeded in moving using peristaltic crawling. The robot could excavate to a depth of 430 mm, i.e., deeper than the excavation unit alone. The maximum torque was kept to less than 10 Nm, which was about 40% less than that of the excavating unit alone and favorable for overall robot motion. Furthermore, except for those few seconds at this relatively large motor torque, motor torque was further reduced by more than 70% during the almost one hour experiment.

Fig. 6 shows the experimental results, in terms of depth with respect to elapsed time, for the four excavation conditions used in the experiment. The average velocity of excavation was 0.19 mm/s at 52 N, 0.19 mm/s at 26 N, 0.23 mm/s at 13 N and 0.21 mm/s at 8.7 N. The average velocities for cases in which the experimental mass was 1/4 and 1/6 of the robot's weight, were similar to the target velocity of 0.25 mm/s. But the velocities at 1/2 and 1/1 of the robot's weight were lower. We believe this occurred because discharged soil fell into the excavated hole and prevented the propulsion unit from working properly. However, the excavator could bore to a depth of around 430 mm, and was expected to be able to excavate deeper because the excavation velocity did not decline except when progressing under its own full weight. Slippage was also observed as the motor torque increased, but the average motor torque was reduced to less than 5 Nm.

Through experiments, it was confirmed that the excavator was able to excavate and move at 1/6 of its own weight. Therefore, it was concluded that the propulsion unit could maintain its body position and rotation for the most part, thereby reducing the effect of the pressure of the surrounding earth in terms of controlling "wall holding" during downwards movement. The EA can effectively make a front space with excavating, transporting and discharging. Both the developed propulsion and excavation units proved effective for use in the prototype excavation robot.

【Development of a Prototype Discharging Part】

The prototype subsurface explorer robot was not equipped with a discharging part, which hindered excavation deeper than 430 mm when the discharge spouts of the robot reached the surface of the ground. Therefore, a discharging part that can transport discharged soil from spouts to the ground was developed. Fig. 7 illustrates the motion of the discharging part. It consists of a winder, bucket and base part. Soil discharged from the spout is collected in a mobile bucket that can be rewound by the winder. The rewound bucket above ejects the soil away from the excavated hole. Wires are connected the bucket to the base part that is fixed to the robot. The base part has two flat spiral springs inside that pull the bucket downward. The winder returns the empty bucket to the base part. The reasons for adopting the flat spiral springs are low-gravity use, simple mechanism and easily adding a sealing mechanism. Fig. 8 shows the excavation experiments of the robot with the developed discharging part. The robot successfully excavated to a depth of 595 mm. When the discharging part is in the soil, the underneath of its spout is below the surface. Thus, it was confirmed that the discharging unit could carry the discharged soil when combined with an excavation robot. However, the experiment was terminated at a depth of 595 mm because of problems with the propulsion unit, probably caused by soil falling from the base part. Thus, it is expected that if the amount of dropped soil was decreased, deeper excavation should be possible.

【Basic Experiments for Modeling Cutting Resistance】

Basic experiments were conducted to reveal the excavation process and rate of cutting torque on the EA for modeling the excavation torque for future use. Excavation resistance is defined as the resistance when the EA of the excavation unit

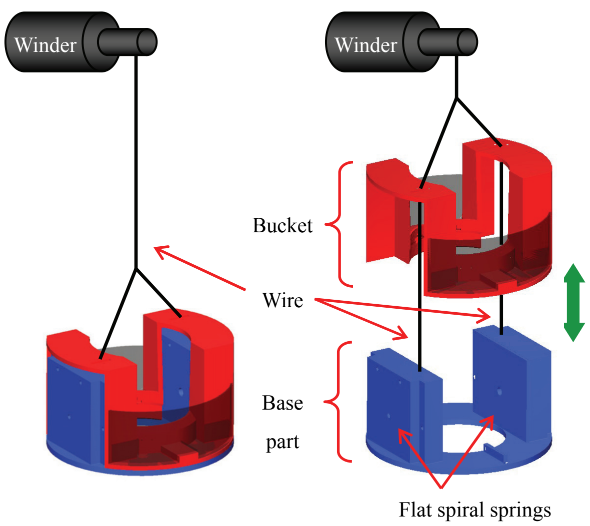

a) While discharging soil b) Winding the bucket

Fig. 7 Motion of discharging part

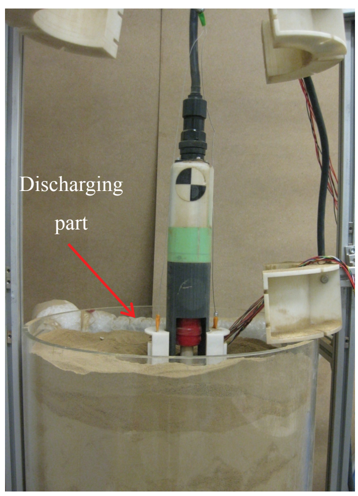

Fig. 8 Excavation experimental results (595 mm)

excavates, transports and discharges. Cutting resistance, which is part of excavation resistance, works at the head of the EA composed of a fish tail (FT) and a screw part with bits, in front of the excavation support.

In the actual cutting process, the EA moves at an angle, because it is continuously moving with tiny rotational and downward movements. The downward movement is set before the beginning of the cutting experiments. Three cutting experiments (Fig. 9) were carried out to reveal the excavation process: (a) Pushing force experiments, (b) Depth experiments, (c) FT cutting experiments.

Table 1 shows the experimental results in terms of maximum torque and torque rate. When the total pushing force is small, depth and pushing force have an equal effect on torque rate. When the pushing force is large, it has a great effect than depth on torque rate. Future cutting models would be calculated taking these results into consideration.

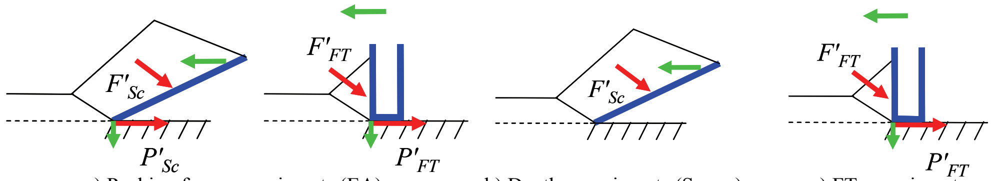

a) Pushing force experiments (EA)　　b) Depth experiments (Screw)　　c) FT experiments

Fig.9 Different patterns of experiments

Table 1 Torque of the FT against the EA

(The number after "P" indicates pushing force e.g., P60: Pushing force of 60 N.)

EA			Screw			Fish tail		
Experiments	Max. torque [Nm]	Torque rate [%]	Depth [mm]	Max. torque [Nm]	Torque rate [%]	Experiments	Max. torque [Nm]	Torque rate [%]
P60	0.27	30	5	0.09	33	P34	0.10	37
P160	0.62	53	10	0.16	26	P66	0.13	21
P260	1.26					P93	0.19	15

【Conclusion and Future Work】

The developed subsurface explorer based on peristaltic crawling of an earthworm as a propulsion unit and an earth auger as an excavation unit successfully excavated to a depth of 430 mm regardless of planetary gravity. The discharging part was improved for deeper excavation, then the robot equipped with that part could excavate to a depth of around 600 mm. In the end, basic cutting experiments at the front of the earth auger were conducted, which showed the rate of excavation torque on the earth auger. In the future, the cutting process would be modeled and the robot would conduct excavation experiments in lunar regolith and Martian simulant. Finally, the robot would be equipped with scientific devices e.g. sampler and seismometer. Moreover, strategies and mechanisms for changing excavation direction would be invented.

【References】

[1] L. Richter, P. Coste, V.V. Gromov, H. Kochan, R. Nadalini, T.C. Ng, S. Pinna , H.-E. Richter, and K.L. Yung, "Development and testing of subsurface sampling devices for the Beagle 2 lander," *Planet. and Space Sci.*, vol. 50, pp. 903–913, Aug. 2002.

[2] C. Stoker, A. Gonzales, J. Zavaleta, "Moon/Mars Underground Mole," *presented at the NASA Sci. Technol. Conf.*, Adelphi, Adelphi, MD, 2007.

[3] K. Zancy, L. Beegle, B. Mellerowicz, S. Sadick, X. Bao and G. Paulsen et al., "Wireline Deep Drill for Exploration of Mars, Europa, and Enceladus," in *Proc. IEEE Aerospace Conference*, Big Sky, MT, 2013, pp.1–14.

[4] K. Yoshida, N. Mizuno, T. Yokoyama, H. Kanamori, M. Sonoyama, and T. Watabe, "Development of a mole-type robot for lunar / planetary subsurface exploration, and its performance evaluation," *presented at the. 20th Annu. Conf. Robot. Soc. of Jpn.*, Osaka, Japan, 2002, Paper 1J35.

[5] K. Nagaoka, T. Kubota, M. Otsuki, and S. Tanaka, "Robotic screw explorer for lunar subsurface investigation: Dynamics modelling and experimental validation," in *Proc. Int. Conf. Adv. Robot.*, Munich, Germany, 2009, pp. 1–6.

[6] Watanabe, K., Shimoda, T., Kubota, T. and Nakatani, A. "A Mole-Type Drilling Robot for Lunar Subsurface Exploration," in *Proc. of 7th Int. Symp. Artificial Intell.*, Robotics and Automation in Space, 2003, AS–7.

[6] S. Yasuda, K. Komatsu, S. Tanaka, "Self-Turning Screw Mechanism for Burying Geophysical Sensors Under Regolith," in *Proc. Int. Symp. Robot.*, Turin, Italy, 2012, 09B02.

[7] H. Omori, T. Murakami, H. Nagai, T. Nakamura, and T. Kubota, "Development of a Novel Bio-Inspired Planetary Subsurface Explorer: Initial Experimental Study by Prototype Excavator With Propulsion and Excavation Units," *IEEE/ASME Transactions on Mechatronics*, vol. 18, no. 2, pp 459–470, April 2013.